Journal of Advanced Zoology

ISSN: 0253-7214

*Volume **44** Issue **3 Year 2023** Page **263:270***

A Comparison of Pre-Trained Models for Pneumonia Disease Prediction Using Chest Images

B. V. Ramana[1*], K. Kavitha[2], G. V. L. Narayana[3], Reventh Raj[4], Naresh Tangudu[5], B. Manideep[6]

*[1'2'3'4'5] Dept. of IT, Aditya Institute of Technology and Management, Tekkali-532201, Srikakulam, A.P, India. ramana.bendi@gmail.com *; [2] kavitha.akki@adityatekkali.edu.in; [3]gvlnarayana.it@ adityatekkali.edu.in; [4]reventh.techie@gmail.com; [5]itsajs@gmail.com.*

[6]Dept. of CSE, Aditya Institute of Technology and Management, Tekkali-532201, Srikakulam, A.P, India. [6]bendimanideep@gmail.com.

**Corresponding author's E-mail: ramana.bendi@gmail.com*

Article History

Received: 06 June 2023
Revised: 15 August 2023
Accepted:21Sept 2023

Abstract

***Aim**: As viral diseases like Corona spread from one person to another, it has great impact on the public health system and socio-economic activities all over the world. **Material and method**: The only way to solve the spreading of this disease is early diagnosis of this disease. **Statistics and Result:** Deep learning algorithms were utilized in this study for comparative analysis of pre-trained models such as VGG16, MobileNetV2 for the detection of pneumonia using different hyper parameters such as batch-size, learning rate, epochs and so on. The proposed models that are MobileNetV2 and VGG16 attains better performance.*

Keywords: *Deep learning, Chest X-ray images, Pneumonia, Disease Prediction, Performance.*

1. Introduction

The corona virus has been linked to cases of severe acute respiratory syndrome. The clinical symptoms of pneumonia infected patients are identical to the signs of illness caused by bacterial pneumonia (Lu et al., 2020; WHO, 2020). The rise in instances was brought on by direct contact between individuals via respiratory droplets (Chavez ET AL., 2020; Corman et al., 2020). Chest X-ray images are frequently employed in the detection of lung illnesses (Guo et al., 2020; Lijens et al., 2017). due to its low cost and less radiation. In this study Deep learning architectures (Cheng et al., 2016; Lakshmanaprabu et al., 2019), such as VGG16 and MobileNet-V2 utilized and evaluated on chest X-ray image dataset.

VGG16 Architecture:

One of the Convolution Neural Network models is the VGG16 model, which has 16 layers. It has layers that are fully linked, fully pooled, max pooled, and convolutional. Fig. 1 mentions the VGG16 architectural block diagram.

MobileNetV2 Architecture:

MobileNetV2 is one of the convolutional neural networks (Alqudah et al., 2020; Alqudah et al., 2019) model and consists of 54 layers. Depth-wise separable convolution is used as building blocks of the model. It has two types of blocks and three layers. One-to-one convolution with ReLU makes up the first layer. The second layer employs a 3X3 depth-wise convolution. Again, linear 1 1 convolution is used in the third layer. There is no ReLU used in the third layer. The MobileNet-V2 is depicted in fig 2.

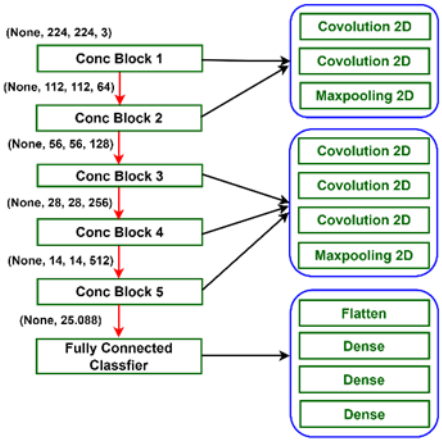

Fig.1. VGG16 Architecture

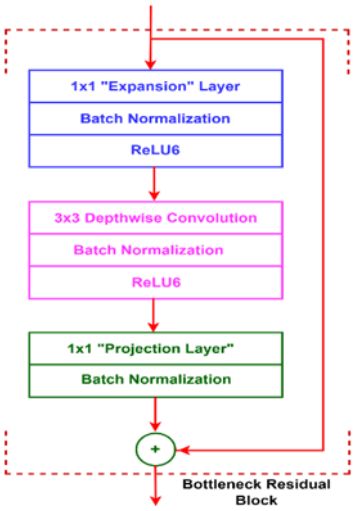

Fig.2. MobileNetV2 Architecture

In MobileNetV2, each layer is represented as a collection of n iterations of one or more related layers. All layers with the same series have the same number of output channels. The complete architecture of MobileNetV2 is represented in fig.3.

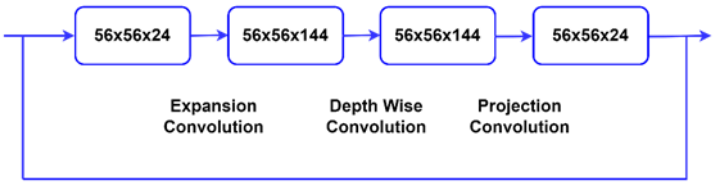

Fig.3. Overall architecture of the MobileNetV2

Related Work

Moutounet-Cartan et.al. (2020) investigated deep neural network models of the VGG16 and VGG19 for the detection of pneumonia infection from chest X-ray images. Khan et. al. (2020) proposed coronet model for accurate diagnosis pneumonia patients by CT images. Wu et al. (2020) established a model on chest CT images and it shows better performance. Deep learning frameworks have been widely used for the detection of pneumonia throughout the past few years (Bhandary et al., 2020; Kermany et al., 2018). Hashmi et al. introduced a novel approach based on a weighted classifier, which combines the weighted predictions from the state-of-the-art deep learning models such as ResNet18, Xception, InceptionV3, DenseNet121, and MobileNetV3 (Hasmi et al., 2020). employed deep transfer learning models GoogLeNet, ResNet-18, and DenseNet-121 (Kundu et al., 2021). Many

authors proposed various ensemble transfer learning models for analyzing X-ray images (Chouhan et al., 2020; Jain et al., 2020).

2. Materials And Methods

Framework suggested for distinguishing pneumonia infection from X-ray images as follows. The framework for disease diagnosis is depicted in fig 4.

Dataset Description

The image dataset was considered from the Kaggle pneumonia X-ray dataset. It encompasses 3000 "X-ray images" of which 1500 are "pneumonia X- Ray images" and 1500 are "Normal X-ray images". The "normal X-ray images" and "pneumonia X- Ray images" are represented in fig 5a and fig 5b respectively.

Fig 5a. Normal X-ray images

Fig 5b. pneumonia X-ray images

Data Pre-processing

Images are pre-processed to improve image quality and to reduce the noise. It includes image resizing, image normalization, data augmentation, data splitting and transfer learning techniques were utilized for enhancing the quality of image and for enhanced performance.

3. Results and Discussion

In this study deep learning techniques were analyzed on the image dataset with performance parameters. Evaluating the Performance of the techniques based on the parameters like accuracy, precision, recall, F1 score and specificity. Confusion matrix is utilized for evaluating the metrics based on actual class and predicted class. The performance metrics are evaluated as follows:

- Accuracy = "TP + TN" / "TP + TN + FP + FN".
- Precision = "TP" / "TP + FP".
- Recall = "TP" / "TP + FN".
- F1 Score = "2 X TP" / "2 X TP + FP + FN".
- Specificity = "TN" / "TN + FP".

VGG16 analysis with performance evaluators is represented in table 1. It achieved "accuracy" of 92%, "specificity" of 96% and "sensitivity" of 89% for epochs 50 and "accuracy" of 95%, "specificity" of 94% and "sensitivity" of 97% for epochs 75 and "accuracy" of 93%, "specificity" of 95% and "sensitivity" of 90% for epochs 100 respectively.

Table 1: **VGG16 Analysis**

Model	Epochs	Batch size	Learning rate	Accuracy	F1- score	Recall	Specificity	Sensitivity
VGG 16	50	8	0.01	0.92	0.93	0.93	0.96	0.89
	75	8	0.01	0.95	0.96	0.96	0.94	0.97
	100	8	0.01	0.93	0.93	0.93	0.95	0.90

The MobileNetV2 analysis with performance evaluators is represented in table 2. It achieved "accuracy" of 96%, "specificity" of 95% and "sensitivity" of 96% for epochs 50 and "accuracy" of 95%, "specificity" of 97% and "sensitivity" of 93% for epochs 75 and "accuracy" of 92%, "specificity" of 91% and "sensitivity" of 91% for epochs 100 respectively.

Table 2: **MobileNetV2 Analysis**

Model	Epochs	Batch size	Learning rate	Accuracy	F1-score	Recall	Specificity	Sensitivity
MobileNet V2	50	8	0.01	0.96	0.96	0.96	0.95	0.96
	75	8	0.01	0.95	0.95	0.95	0.97	0.93
	100	8	0.01	0.92	0.92	0.92	0.91	0.91

MobileNetV2 indicates greatest "accuracy" of 96%, "sensitivity" of 96%, "specificity" of 97% and average of recall and f1score of 96% when it is compared with the VGG16 model based on table 1 and table 2. Sample confusion matrix represented in fig 6.

Confusion Matrices for the VGG16 model with epochs 50, 75 and 100 were represented in fig-7, fig-8 and fig-9. Similarly, confusion Matrices for the MobileNetV2 model with epochs 50, 75 and 100 were represented in fig-10, fig-11 and fig-12 respectively. The confusion matrix values for VGG16 and MobileNetV2 are represented in table 3.

	Predicted 0	Predicted 1
Actual 0	TN	FP
Actual 1	FN	TP

Fig 6. Confusion Matrix

Table 3: **Confusion matrix values of VGG 16 and MobileNetV2 Analysis**

	VGG 16			MobileNetV2		
	Epoch-50	Epoch-75	Epoch-100	Epoch-50	Epoch-75	Epoch-100
TP	290	290	290	290	290	290
FP	10	20	11	10	20	11
FN	14	9	8	14	9	7
TN	290	280	290	290	280	290

In table 3 for the VGG16 model of Epoch 50 has identified 290 images as pneumonia infected images, while 10 of the pneumonia class images were incorrectly classified. 14 images were incorrectly recognized as pneumonia images whereas 290 images in normal were appropriately identified as normal images.

Accuracy and loss metrics are used for analyzing models about their performance. The loss and accuracy curve for VGG16 model with epochs 50, 75 and 100 are designated in fig-13, fig-14 and fig-15 respectively. The loss and accuracy curve for MobileNetV2 model with epochs 50, 75 and 100 are represented in fig-16, fig-17 and fig-18 respectively.

The loss and accuracy metrics are also used for the performance evaluation of models. High accuracy and minimum loss are required for greater performance that is represented in fig-19. The "loss" and "accuracy" values for both "training" and "validation" for VGG 16 and MobileNetV2 models for epoch 50, 75 and 100 are evaluated and represented in table 4.

VGG16 and MobileNetV2 models are analyzed based on their accuracy, specificity, and sensitivity for epoch 50, 75 and 100 with learning rate 1 and batch size of 8 and training and testing ratio is 80:20 and represented in table 5. VGG 16 analysis is represented graphically in fig-20, fig-21 and fig-22. Whereas MobileNetV2 analysis is represented graphically in fig-23, fig-24 and fig- 25.

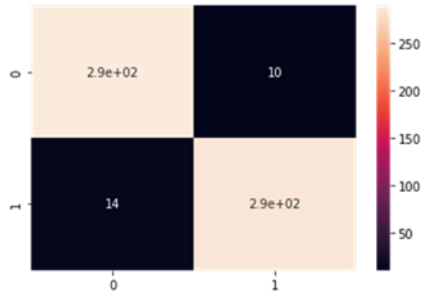

Fig 7. Confusion Matrices of VGG16 with Epochs 50

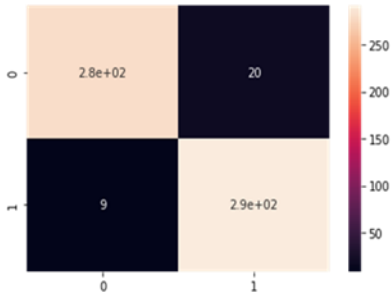

Fig 8. Confusion Matrices of VGG16 with Epochs 75

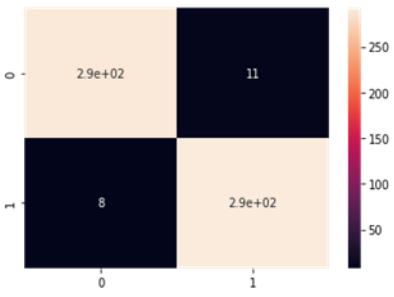

Fig 9. Confusion Matrices of VGG16 with Epochs 100

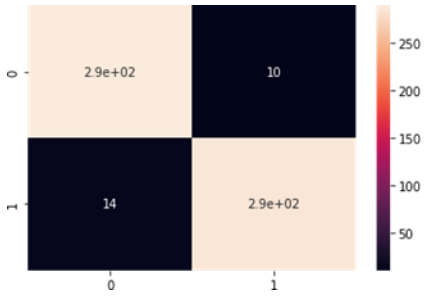

Fig 10. MobileNetV2 with Epochs 50

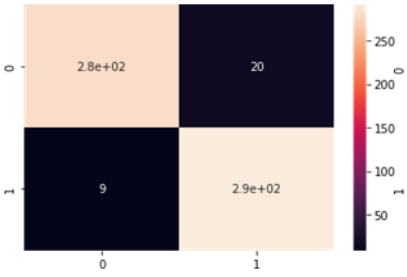

Fig 11. Confusion Matrices of MobileNetV2 with Epochs 75

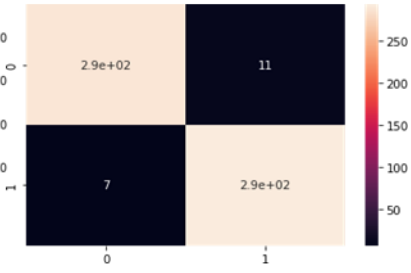

Fig 12. Confusion Matrices of MobileNetV2 with Epochs 100

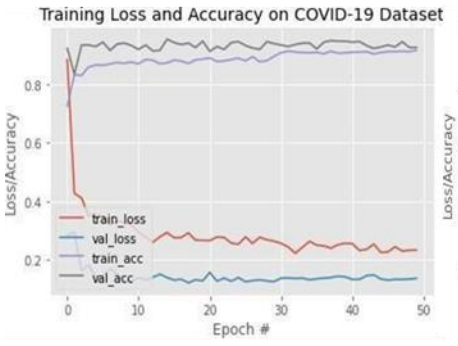

Fig 13. VGG16 Loss/Accuracy for Epoch 50

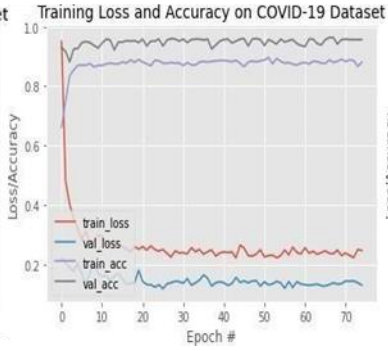

Fig 14. VGG16 Loss/Accuracy for Epoch 75

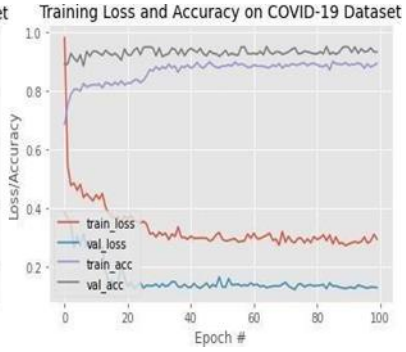

Fig 15. VGG16 Loss/Accuracy for Epoch 100

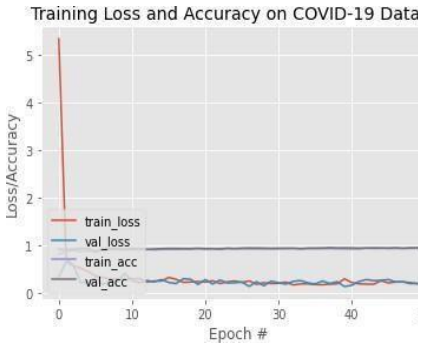

Fig 16. MobileNetV2 Loss/Accuracy for Epoch 50

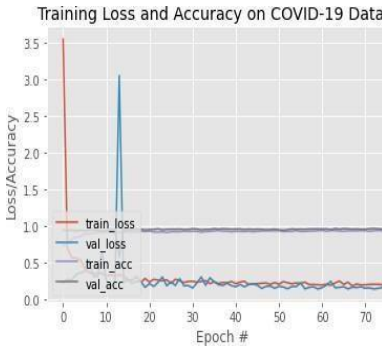

Fig 17. MobileNetV2 Loss/Accuracy for Epoch 75

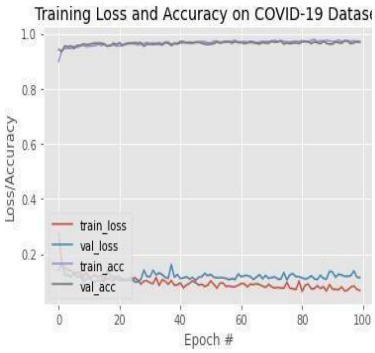

Fig 18. MobileNetV2 Loss/Accuracy for Epoch 100

Fig 19. Loss and Accuracy Matrix

	Low Loss	**High Loss**
Low Accuracy	A lot of small errors	A lot of big errors
High Accuracy	A few small errors	A few big errors

Table 4: Loss and Accuracy values of VGG 16 and MobileNetV2 Analysis

	VGG 16			**MobileNetV2**		
	Epoch-50	**Epoch-75**	**Epoch-100**	**Epoch-50**	**Epoch-75**	**Epoch-100**
Train Accuracy	91	88	93	91	93	97
Validation Accuracy	92	95	89	95	95	96
Train Loss	0.23	0.24	0.29	0.21	0.19	0.06
Validation Loss	0.13	0.13	0.13	0.20	0.15	0.11

Table 5: Comparison of VGG 16 and MobileNetV2 Analysis

	VGG 16			**MobileNetV2**		
	Epoch-50	**Epoch-75**	**Epoch-100**	**Epoch-50**	**Epoch-75**	**Epoch-100**
Accuracy	92	95	93	96	95	96
Specificity	96	94	95	95	97	97
Sensitivity	89	97	90	96	93	96

VGG 16 has the highest accuracy for epoch 75, highest specificity for epoch 50 and highest sensitivity for epoch 75. Whereas MobileNetV2 has the highest accuracy for epoch 50 & 100, highest specificity for epoch 75 & 100 and highest sensitivity for epoch 50 & 100. VGG16 and MobileNetV2 models are compared for epoch 50, 75 and 100 represented in fig 26, fig 27 and fig 28 respectively.

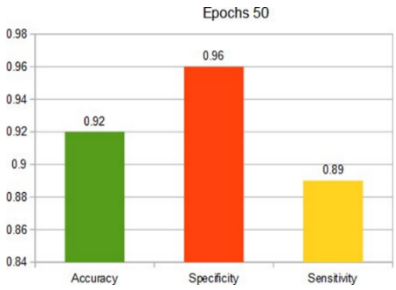

Fig. 20. VGG16 with Epoch 50

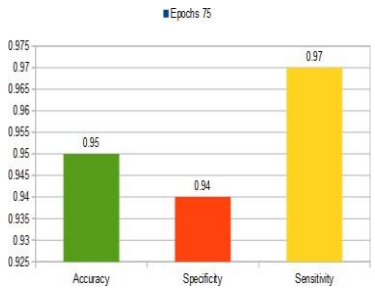

Fig. 21. VGG16 with Epoch 75

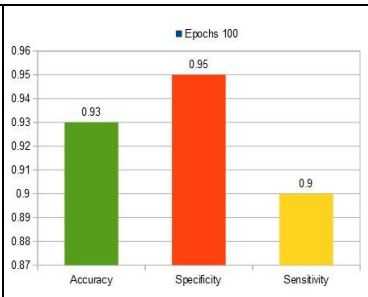

Fig. 22. VGG16 with Epoch 100

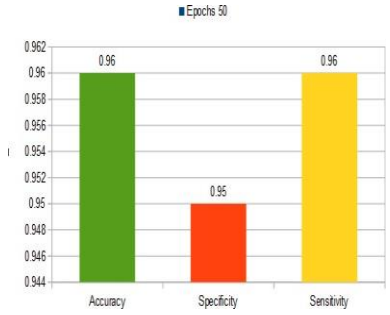

Fig. 23. MobileNetV2 with Epoch 50

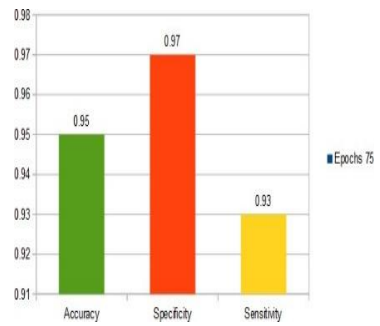

Fig.24. MobileNetV2 with Epoch 75

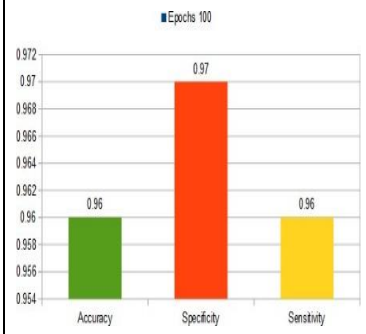

Fig.25.MobileNetV2 with Epoch 10

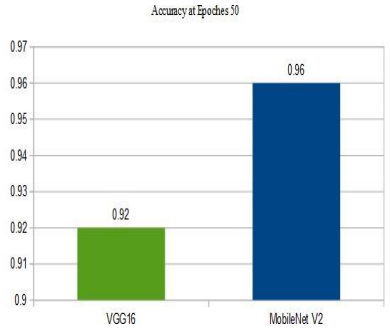

Fig. 26. Comparative Analysis of Models with Epochs 50

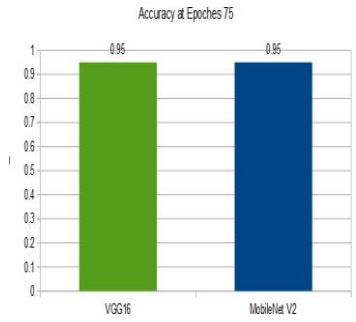

Fig. 27. Comparative Analysis of Models with Epochs 75

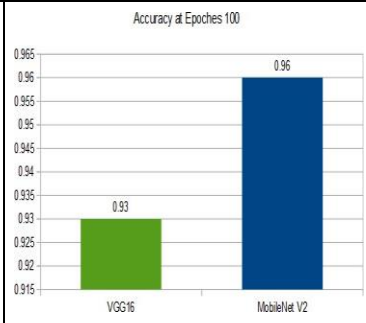

Fig.28. Comparative Analysis of Models with Epochs 100

4. Conclusion

The efficient detection of pneumonia infection due to Carona virus is possible by analyzing images. In this study “VGG16” and “MobileNetV2” were considered for the detection of the “pneumonia X-ray images” from “pneumonia X-ray images”. The effectiveness has been improved with data pre-processing, augmentation and transfer learning techniques by enhancing visual quality of the image. Performance of these models were evaluated based on Precision, recall, F1score, and accuracy. Performance has been validated with pneumonia dataset consisting of 1500 “pneumonia X-ray images” and 1500 “normal X-ray images”. MobileNetV2 model achieved “accuracy” of 96%, “sensitivity” of 96% and “specificity” of 95%.

References:

Alqudah, A. M., Alquraan, H., & Qasmieh, I. A. (2019). Segmented and non-segmented skin lesions classification using transfer learning and adaptive moment learning rate technique using pretrained convolutional neural network. *Journal of Biomimetics, Biomaterials and Biomedical Engineering, 42*, 67-78. https://doi.org/10.4028/www.scientific.net/JBBBE.42.67

Alqudah, A. M., Qazan, S., & Alqudah, A. (2020). Automated systems for detection of COVID-19 using chest X-ray images and lightweight convolutional neural networks. https://doi.org/10.21203/rs.3.rs-17262/v1

Bhandary, A., Prabhu, G. A., Rajinikanth, V., Thanaraj, K. P., Satapathy, S. C., Robbins, D. E., ... Raja, N. S. M. (2020). Deep-learning framework to detect lung abnormality–A study with chest X-Ray and lung CT scan images. *Pattern Recognition Letters*, *129*, 271-278. https://doi.org/10.1016/j.patrec.2019.09.019

Chavez, S., et al. (2020). Coronavirus Disease (pneumonia-19): A primer for emergency physicians. *American Journal of Emergency Medicine*. https://doi.org/10.1016/j.ajem.2020.03.036

Cheng, J. Z., Ni, D., Chou, Y. H., Qin, J., Tiu, C. M., Chang, Y. C., ... Chen, C. M. (2016). Computer-aided diagnosis with deep learning architecture: Applications to breast lesions in US images and pulmonary nodules in CT scans. *Scientific Reports*, *6*(1), 24454. https://doi.org/10.1038/srep24454

Chouhan, V., Singh, S. K., Khamparia, A., Gupta, D., Tiwari, P., Moreira, C., ... De Albuquerque, V. H. C. (2020). A novel transfer learning-based approach for pneumonia detection in chest X-ray images. *Applied Sciences*, *10*(2), 559. https://doi.org/10.3390/app10020559

Corman, V. M., Landt, O., Kaiser, M., Molenkamp, R., Meijer, A., Chu, D. K., ... Mulders, D. G. (2020). Detection of 2019 novel coronavirus (2019-nCoV) by real-time RT-PCR. *Eurosurveillance*, *25*(3), 2000045. https://doi.org/10.2807/1560-7917.ES.2020.25.3.2000045

Goyal, S. and Singh, R. (2021). Detection and classification of lung diseases for pneumonia and Covid-19 using machine and deep learning techniques. *Journal of Ambient Intelligence and Humanized Computing*. https://doi.org/10.1007/s12652-021-03226-y

Guo, Y. R., Cao, Q. D., Hong, Z. S., Tan, Y. Y., Chen, S. D., Jin, H. J., ... Yan, Y. (2020). The origin, transmission and clinical therapies on coronavirus disease 2019 (COVID-19) outbreak–an update on the status. *Military Medical Research*, *7*, 1-10. https://doi.org/10.1186/s40779-020-00240-0

Hammoudi, K., Benhabiles, H., Melkemi, M., Dornaika, F., Arganda-Carreras, I., Collard, D., & Scherpereel, A. (2021). Deep learning on chest X-ray images to detect and evaluate pneumonia cases at the era of COVID-19. *Journal of medical systems*, *45*(7), p.75. https://doi.org/10.1007/s10916-021-01769-1

Hashmi, M. F., Katiyar, S., Keskar, A. G., Bokde, N. D., & Geem, Z. W. (2020). Efficient pneumonia detection in chest X-ray images using deep transfer learning. *Diagnostics*, *10*(6), 417. https://doi.org/10.3390/diagnostics10060417

Huang, C., Wang, Y., Li, X., Ren, L., Zhao, J., Hu, Y., ... Cheng, Z. (2020). Clinical features of patients infected with 2019 novel coronavirus in Wuhan, China. *The Lancet*, *395*(10223), 497-506. https://doi.org/10.1016/S0140-6736(20)30183-5

Ibrahim, A.U., Ozsoz, M., Serte, S., Al-Turjman, F. and Yakoi, P.S. (2021). Pneumonia classification using deep learning from chest X-ray images during COVID-19. *Cognitive Computation*. https://doi.org/10.1007/s12559-021-09955-3

Jain, R., Nagrath, P., Kataria, G., Kaushik, V.S. and Hemanth, D.J. (2020). Pneumonia detection in chest X-ray images using convolutional neural networks and transfer learning. *Measurement*, *165*, p.108046. https://doi.org/10.1016/j.measurement.2020.108046](https://doi.org

Kermany, D. S., Goldbaum, M., Cai, W., Valentim, C. C., Liang, H., Baxter, S. L., ... Dong, J. (2018). Identifying medical diagnoses and treatable diseases by image-based deep learning. *Cell*, *172*(5), 1122-1131. https://doi.org/10.1016/j.cell.2018.02.010

Khan, A. I., Shah, J. L., & Bhat, M. M. (2020). CoroNet: A deep neural network for detection and diagnosis of COVID-19 from chest X-ray images. *Computer Methods and Programs in Biomedicine*, *196*, 105581. https://doi.org/10.1016/j.cmpb.2020.105581

Kundu, R., Das, R., Geem, Z. W., Han, G. T., & Sarkar, R. (2021). *PLoS ONE*, *16*(9), e0256630. https://doi.org/10.1371/journal.pone.0256630

Lai, C. C., Shih, T. P., Ko, W. C., Tang, H. J., & Hsueh, P. R. (2020). Severe acute respiratory syndrome coronavirus 2 (SARS-CoV-2) and coronavirus disease-2019 (COVID-19): The epidemic and the challenges. *International Journal of Antimicrobial Agents*, *55*(3), 105924. https://doi.org/10.1016/j.ijantimicag.2020.105924

Lakshmanaprabu, S. K., Mohanty, S. N., Shankar, K., Arunkumar, N., & Ramirez, G. (2019). Optimal deep learning model for classification of lung cancer on CT images. *Future Generation Computer Systems*, *92*, 374-382. https://doi.org/10.1016/j.future.2018.09.037

Litjens, G., Kooi, T., Bejnordi, B. E., Setio, A. A. A., Ciompi, F., Ghafoorian, M., ... Sánchez, C. I. (2017). A survey on deep learning in medical image analysis. *Medical Image Analysis*, *42*, 60-88. https://doi.org/10.1016/j.media.2017.07.005

Lu, H., Stratton, C. W., & Tang, Y. W. (2020). Outbreak of pneumonia of unknown etiology in Wuhan, China: The mystery and the miracle. *Journal of Medical Virology*, *92*(4), 401. https://doi.org/10.1002/jmv.25678

Moutounet-Cartan, P. G. (2020). Deep convolutional neural networks to diagnose COVID-19 and other pneumonia diseases from posteroanterior chest X-rays. https://arxiv.org/abs/2005.00845

Wang, W., Xu, Y., Gao, R., Lu, R., Han, K., Wu, G., & Tan, W. (2020). Detection of SARS-CoV-2 in different types of clinical specimens. *JAMA*, *323*(18), 1843-1844. https://doi.org/10.1001/jama.2020.3786

World Health Organization. (2020). Laboratory testing for coronavirus disease 2019 (COVID-19) in suspected human cases: Interim guidance, 2 March 2020 (No. WHO/COVID-19/laboratory/2020.4). https://www.who.int/publications/i/item/WHO-2019-nCoV-laboratory-2020.4

Wu, X., Hui, H., Niu, M., Li, L., Wang, L., He, B., ... Zha, Y. (2020). Deep learning-based multi-view fusion model for screening 2019 novel coronavirus pneumonia: A multicentre study. *European Journal of Radiology*, *128*, 109041. https://doi.org/10.1016/j.ejrad.2020.109041